Microcracking in piezoelectric materials by the Boundary Element Method

I. Benedetti[1,a], V. Gulizzi[1,b] and A. Milazzo[1,c]

[1]Dipartimento di Ingegneria

Università degli Studi di Palermo, Viale delle Scienze, Edificio 8, 90128, Palermo, Italy

[a]ivano.benedetti@unipa.it, [b]vincenzo.gulizzi@unipa.it, [c]alberto.milazzo@unipa.it

Keywords: Boundary Element Method, Microcracking, Piezoelectric ceramics, Polycrystalline materials

Abstract. A 3D boundary element model for piezoelectric polycrystalline micro-cracking is discussed in this contribution. The model is based on the boundary integral representation of the electro-mechanical behavior of individual grains and on the use of a generalized cohesive formulation for inter-granular micro-cracking. The boundary integral formulation allows to address the electro-mechanical boundary value problem in terms of generalized grain boundary and inter-granular displacements and tractions only, which implies the natural inclusion of the cohesive laws in the formulation, the simplification of the analysis pre-processing stage, and the reduction of the number of degrees of freedom of the overall analysis with respect to other popular numerical methods.

Introduction

Piezoelectric ceramics are widely employed in the manufacturing of transducers for disparate engineering applications, such as Structural Health Monitoring (SHM) and micro electro-mechanical devices (MEMS) [1-5]. In such applications, their inherent brittleness may favor the progressive deterioration and micro-cracking of the piezoelectric components. For such a reason, the availability of reliable modelling and simulation tools may be of relevant engineering interest.

Recent trends in materials micro-characterization and high performance computing (HPC) have allowed better understanding of the behavior of heterogeneous materials at the constituents scale, thus enhancing the understanding of the link between the microstructure and macroscopic properties [6]. In this context, polycrystalline materials, among others, have been widely investigated and provide a typical example of heterogeneous materials.

Polycrystalline materials have been extensively studied by means of the finite element method (FEM) [7], whereas the literature about numerical modelling of piezoelectric polycrystals more limited [8]. In computational micromechanics, a drawback of FE methods is induced by the high number of degrees of freedom required to tackle the boundary value problem, especially in the case of three-dimensional modelling.

The boundary element method (BEM) offers an effective alternative to the more popular FEM in several modelling applications. The hallmark feature of the BEM is the expression of the considered boundary value problem in terms of boundary unknowns only [9]. BEM models have been successfully applied to the study of polycrystalline mechanics and micro-cracking [10,11,12,13,14,15,16]. Also concurrent two-scale models where macroscopic damage is extracted from explicit microscopic simulations of polycrystalline materials are available in the literature [17,18] and exemplify the effectiveness and capabilities of BEM approaches. BEM has also been employed to model piezoelectric bodies and for fracture mechanics problems [19,20].

In this work, a boundary element formulation for piezoelectric polycrystalline micro-cracking is discussed. The polycrystalline aggregate is represented using Voronoi tessellations and the formulation is based on a BEM multi-region approach where each Voronoi cell represents a piezoelectric grain. To reproduce unpoled and partially poled piezoelectric polycrystals, the grains orientation is given in terms of a prescribed orientation distribution function. The grain interfaces are modeled using suitably defined generalized cohesive laws. The effectiveness of the method in dealing with both computational homogenization and micro-cracking is shown with few numerical applications. The method might find application in the design of MEMS devices and transducers for structural applications.

Boundary Element formulation for polycrystalline piezoelectric materials

The BEM for 3D polycrystalline piezoelectric materials is discussed here. The morphology of polycrystalline aggregates is generated using Voronoi tessellations. The morphology discretization is performed as described in Ref. [21].

The notation and some definitions are given first: $\mathbf{u}=\{u_i\}$ and ϕ denote the displacements field and electric potential, respectively; $\boldsymbol{\sigma}=\{\sigma_{ij}\}$ and $\boldsymbol{\gamma}=\{\gamma_{ij}\}$ are the stress and strain tensors; $\mathbf{E}=\{E_i\}$ and $\mathbf{D}=\{D_i\}$ denote the electric field and electric displacement vectors. Eventually, $\mathbf{t}=\{t_i\}$ and ω denote the boundary tractions and the surface charge density, respectively, which are related to the stress tensor and the electric displacement vector as $t_i=\sigma_{ij}n_j$ and $\omega=-D_in_i$, being n_i the outward unit normal of the considered piezoelectric domain.

Piezoelectric constitutive behavior. Each piezoelectric grain presents the constitutive relationships

$$\begin{aligned}\sigma_{ij}&=c^E_{ijkl}\gamma_{kl}-e_{kij}E_k\\ D_i&=e_{ikl}\gamma_{kl}+\kappa^\gamma_{ij}E_j\end{aligned} \tag{1}$$

where c^E_{ijkl}, e_{ikl} and κ^γ_{ij} are the elasticity tensor at constant electric field, the piezoelectric coupling tensor and the dielectric tensor at constant strain, respectively. Implicit summation is assumed over repeated subscripts.

Grain governing equations and boundary element formulation. In absence of body forces and volume free electric charges, the governing equations of piezoelectric media are the mechanical equilibrium and the Gauss' law for electrostatics, which read

$$\sigma_{ij,j}=0 \quad \textit{mechanical equilibrium}, \qquad D_{i,i}=0 \quad \textit{Gauss' laws} \tag{2}$$

where the comma in the subscripts denotes differentiation with respect to the index following the comma itself. The above equations are coupled with the strain-displacement relationships and the electric field-electric potential relationship

$$\gamma_{ij}=(u_{i,j}+u_{j,i})/2 \quad \text{and} \quad E_i=-\phi_{,i} \tag{3}$$

It can be shown [19] that the above equations can be recast in the following unified boundary integral form

$$c_{ij}(\mathbf{y})U_j(\mathbf{y})+\int_S T^*_{ij}(\mathbf{x},\mathbf{y})U_j(\mathbf{x})\mathrm{d}S(\mathbf{x})=\int_S U^*_{ij}(\mathbf{x},\mathbf{y})T_j(\mathbf{x})\mathrm{d}S(\mathbf{x}), \tag{4}$$

where the generalized notation

$$U_i=\begin{cases}u_i & i\le 3\\ \phi & i=4\end{cases}, \quad \text{and} \quad T_i=\begin{cases}t_i & i\le 3\\ \omega & i=4\end{cases} \tag{5}$$

has been introduced. In Eq.4, S denotes the boundary of the considered piezoelectric domain, **x** and **y** are the integration and collocation points, c_{ij} are the free-terms stemming from the collocation limiting process, and U^*_{ij} and T^*_{ij} are the fundamental solutions of piezoelectricity, computed as in Ref.[22].

Eq.4 holds for the generic piezoelectric grain within the aggregate. Its discrete BEM counterpart is obtained by following the standard discretization, collocation and integration procedures [21].

Interface equations. The inter-granular interfaces within the aggregate are assumed initially pristine, so that electro-mechanical continuity holds at the beginning of the analysis. When the critical condition

$$t_e=\sqrt{\langle t_n\rangle^2+\left(\frac{\alpha_2}{\alpha_1}t_s\right)^2}\ge T_{\max} \tag{6}$$

is reached, a generalized extrinsic cohesive law of the form

$$\begin{bmatrix} t_n \\ t_s \\ D_n \end{bmatrix} = \begin{bmatrix} C_{nn}\left(d^*\right) & 0 & C_{n\phi}\left(d^*\right) \\ 0 & C_{ss}\left(d^*\right) & 0 \\ 0 & 0 & C_{D\phi}\left(d^*\right) \end{bmatrix} \begin{bmatrix} \delta u_n \\ \delta u_s \\ \delta\phi \end{bmatrix} \tag{7}$$

is introduced, where t_n and t_s are the normal and tangential traction components at the interface, D_n is the normal component of the electric displacement vector, δu_n, δu_s and $\delta\phi$ are displacement and electric potential jumps, and

$$C_{nn}\left(d^*\right) = \frac{T_{\max}}{\delta u_{cr}^n}\frac{1-d^*}{d^*}, \qquad C_{ss}\left(d^*\right) = \frac{\alpha_1 T_{\max}}{\delta u_{cr}^s}\frac{1-d^*}{d^*} \tag{8}$$

are the coefficient accounting for the purely mechanical part of the cohesive law, and

$$C_{D\phi}\left(d^*\right) = \frac{\kappa_{gb}\left(d^*\right)}{\delta u_n}, \qquad C_{n\phi}\left(d^*\right) = \frac{\kappa_{gb}\left(d^*\right)}{2}\frac{\delta\phi}{\delta u_n^2} \tag{9}$$

are the terms accounting for the electro-mechanical coupling. In the above equations, δu_{cr}^n and δu_{cr}^s are the critical normal and tangential displacement jumps, κ_{gb} is the grain boundary dielectric permittivity. On the other hand , $d^* \in [0,1]$ is a parameter expressing the irreversible accumulation of damage at the interface, defined as in Ref.[13].

Once the interface is completely failed, the laws of frictional contact, enriched by terms accounting for the electro-static attraction, are introduced to govern its behavior.

Boundary conditions. Different types of boundary conditions can be enforced on the polycrystalline aggregate. In this work, generalized periodic boundary conditions are used for homogenization purposes [23], while standard kinematical boundary conditions are employed for micro-cracking analyses.

Polycrystalline system assembly and solution. The governing equations for the whole aggregate are obtained by writing the discrete counterpart of Eq.4 for each grain and by employing the interface conditions for restoring the continuity of the aggregate. For a N_g -grain aggregate, the resulting system can be written as

$$\begin{bmatrix} \mathbf{H}^{\langle 1\rangle} & \cdots & \mathbf{0} \\ \vdots & \ddots & \vdots \\ \mathbf{0} & \cdots & \mathbf{H}^{\langle N_g\rangle} \\ \leftarrow & \mathbf{I}_U\left(d^*\right) & \rightarrow \end{bmatrix} \begin{Bmatrix} \mathbf{U}^{\langle 1\rangle} \\ \vdots \\ \mathbf{U}^{\langle N_g\rangle} \end{Bmatrix} - \begin{bmatrix} \mathbf{G}^{\langle 1\rangle} & \cdots & \mathbf{0} \\ \vdots & \ddots & \vdots \\ \mathbf{0} & \cdots & \mathbf{G}^{\langle N_g\rangle} \\ \leftarrow & \mathbf{I}_T & \rightarrow \end{bmatrix} \begin{Bmatrix} \mathbf{T}^{\langle 1\rangle} \\ \vdots \\ \mathbf{T}^{\langle N_g\rangle} \end{Bmatrix} = \begin{Bmatrix} \mathbf{0} \\ \vdots \\ \mathbf{0} \\ \mathbf{b} \end{Bmatrix} \tag{10}$$

where: the superscript $\langle g\rangle$ denotes a quantities related to the *g*-th grain, $\mathbf{U}^{\langle g\rangle}$ and $\mathbf{T}^{\langle g\rangle}$ collect the nodal values of the generalized displacements and tractions; $\mathbf{H}^{\langle g\rangle}$ and $\mathbf{G}^{\langle g\rangle}$ stem from the numerical integration of Eq.4; $\mathbf{I}_U\left(d^*\right)$ and $\mathbf{I}_T$ collect the coefficients of the generalized displacements and tractions appearing in the interface equations and periodic boundary conditions and **b** collects the prescribed values appearing on the right-hand side of the periodic boundary conditions. The solution of the sparse system given in Eq.10 follows the same strategy adopted in [21]. A computational sped-up could be obtained by employing hierarchical matrices coupled with iterative solvers [24,25].

Computational tests

The described formulation is employed for the computation homogenization of piezoelectric polycrystalline aggregates and for micro-cracking analysis. Prescribed components of strain and electric fields are enforced and the apparent properties are computed in terms of macroscopic stress field and macroscopic electric displacement field using volume averages as described in Ref.[23].

Computational homogenization. The selected material for the grains is $BaTiO_3$, whose non-zero constitutive constants in the local reference system are taken from [26]. The orientation of the grains within

the aggregate is defined by the three Euler angles α, β and γ according to the ZXZ convention, whose value is randomly chosen by means of three orientation distribution functions. The angles α and γ represent rotation around the Z axis and are assumed to be uniformly distributed in the $[0,2\pi)$ interval. In order to account for un-poled, partially poled and fully poled aggregates, the angle β is assumed to be distributed over the interval $[0,\beta_{\max})$ according to the following probability density function

$$p_\beta(x)=\frac{\sin x}{2\sin^2(\beta_{\max}/2)}, \quad x\in[0,\beta_{\max}), \tag{11}$$

where $\beta_{\max}$ is the maximum angle between the global x_3 direction of the aggregate and the local x_3 axis of each grain: $\beta_{\max}=\pi$ denotes an isotropic (completely random) orientation of the piezoelectric crystals that, in turn, corresponds to a macroscopically un-poled aggregate; $\beta_{\max}=0$ denotes a complete alignment of the grains with the global x_3 direction, i.e. a fully poled state.

Fig.(1) reports about the behavior of some selected constitutive constants as a function of the maximum polarization angle $\beta_{\max}$: each point of the curves is obtained by averaging over ensembles of 100 realizations of 50-grain morphologies. It is noted as the homogenized properties fall within the Voigt and Reuss averages, identified by the grey shaded areas in the plots.

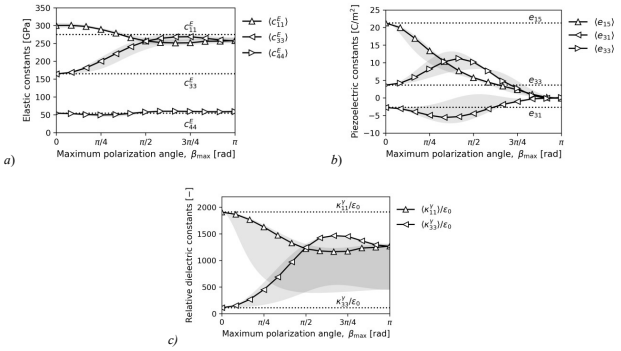

a) *b*) *c*)

Fig.1: Homogenized constitutive properties for $BaTiO_3$ piezoelectric aggregates as a function of the maximum polarization angle $\beta_{\max}$: *a*) selected elastic constants, *b*) selected piezoelectric constants and *c*) selected dielectric constants. The shaded grey regions correspond to the Voigt and Reuss averages.

Micro-cracking analysis. Fig.(2) shows the homogenized component of stress $\bar{\sigma}_{33}$ and the homogenized component of electric displacement $\bar{D}_3$ versus applied strain $\bar{\gamma}_{33}$ for a cubic 100-grain morphology consisting of PZT-4 crystals with average size $d=5$ μm. The constitutive constants for the bulk crystals are taken from [28], whereas the parameters appearing in Eqs.6-9 are selected has follows: $T_{\max}=80$ MPa, $\delta u_{cr}^n=0.05$ μm, $\delta u_{cr}^s=0.1$ μm, $\alpha_1=1$, $\alpha_2=\sqrt{2}$, $\kappa_{gb}=635\varepsilon_0(1-d^*)+\varepsilon_0 d^*$ being ε_0 the vacuum permittivity. For each diagram, the different curves are obtained for different levels of applied electric potential between the top and bottom faces of the morphology. The graphs are obtained by random distribution of β, with the indicated constraint on the maximum polarization angle.

Summary

The application of a generalized boundary element formulation to the computational homogenization and micro-cracking analysis of piezoelectric polycrystalline aggregates is described in this contribution. The developed framework is based on a suitable generalised integral representation of the electro-mechanical boundary value problem coupled with a suitable representation of the inter-granular interfaces, employing generalised cohesive traction-separation laws. The computational homogenization results are in line with analytical predictions and literature data. The micro-cracking results are qualitatively consistent, although further validation would be needed to assess the predictive capability of the method. The developed framework could be a useful tool in the design of transducers and MEMS.

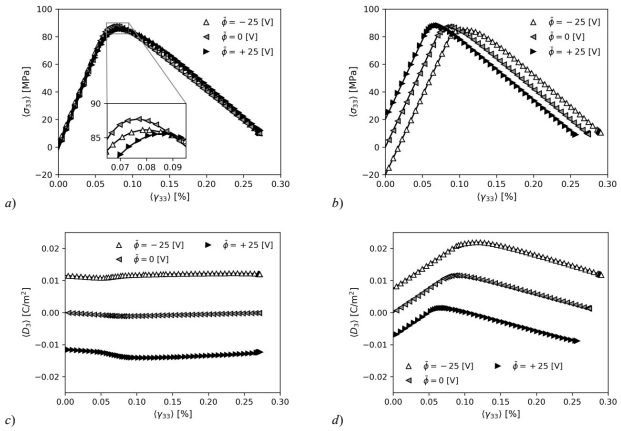

Fig.2: (*a*-*b*) homogenized stress component $\bar{\sigma}_{33}$ and (*c*-*d*) homogenized electric displacement component $\bar{D}_3$ versus applied strain $\bar{\gamma}_{33}$ for a cubic 100-grain morphology with average grain size $d = 5$ μm. For each diagram, the three curves are obtained for three different level of applied electric potential between the top and bottom faces of the morphology. Figures (*a*,*c*) and figures (*b*,*d*) are obtained by random distribution of β, with the constraint on the maximum polarization angle $\beta_{\max} = \pi$ and $\beta_{\max} = 0$, respectively.

References

[1] W. Staszewski, C. Boller and G.R Tomlinson *Health monitoring of aerospace structures: smart sensor technologies and signal processing,* John Wiley & Sons, (2004).
[2] I. Benedetti, M.H. Aliabadi and A. Milazzo *Computer Methods in Applied Mechanics and Engineering*, **199**(9-12), 490-501 (2010).
[3] F. Zou, I. Benedetti, M.H. Aliabadi, *Smart Materials and Structures*, 23(1), 015022, (2013)
[4] V. Gulizzi, P. Rizzo, A. Milazzo. *AIAA Journal*, 53(11), 3479-3483, (2015).
[5] V. Gulizzi, P. Rizzo, A. Milazzo, E.L.M. Ribolla. *Journal of Civil Structural Health Monitoring*,*5*(3), 337-352, (2015).
[6] S. Nemat-Nasser and M. Hori *Micromechanics: Overall Properties of Heterogeneous Materials,* North Holland, (1999).
[7] F. Roters, P. Eisenlohr, L. Hantcherli, D.D. Tjahjanto, T.R. Bieler and D. Raabe. *Acta Materialia*, **58**(4), 1152-1211 (2010).
[8] C.V. Verhoosel and M.A. Gutiérrez *Engineering Fracture Mechanics*, **76**(6), 742-760 (2009).

[9] M.H. Aliabadi *The boundary element method, applications in solids and structures Vol.2,* John Wiley & Sons, (2002).
[10] G.K. Sfantos and M.H. Aliabadi *International Journal of Numerical Methods in Engineering*, **69**(8), 1590-1626 (2007).
[11] G. Geraci and M.H. Aliabadi *Engineering Fracture Mechanics*, **176**, 351-374 (2017).
[12] I. Benedetti and M.H. Aliabadi *Computational Materials Science*, **67**, 249-260 (2013).
[13] I. Benedetti and M.H. Aliabadi *Computer Methods in Applied Mechanics and Engineering*, **265**, 36-62 (2013).
[14] I. Benedetti, V. Gulizzi and V. Mallardo *International Journal of Plasticity*, **83**, 202-224 (2016).
[15] I. Benedetti, V. Gulizzi and A. Milazzo *Mechanics of Materials*, **117**, 137-151 (2018).
[16] V. Gulizzi, C.H. Rycroft and I. Benedetti *Computer Methods in Applied Mechanics and Engineering*, **329**, 168-194 (2018).
[17] G.K. Sfantos and M.H. Aliabadi *Computer Methods in Applied Mechanics and Engineering*, **196**(7), 1310-1329 (2007).
[18] I. Benedetti and M.H. Aliabadi *Computer Methods in Applied Mechanics and Engineering*, **289**(1), 429-453 (2015).
[19] E. Pan *Engineering Analysis with Boundary Elements*, **23**(1), 67-76 (1999).
[20] G. Davi and A. Milazzo *International Journal of Solids and Structures*, **38**(40), 7065-7078 (2001).
[21] V. Gulizzi, A. Milazzo and I. Benedetti *Computational Mechanics*, **56**(4), 631-651 (2015).
[22] V. Gulizzi, A. Milazzo and I. Benedetti *International Journal of Solids and Structures*, **100**, 169-186 (2016).
[23] I. Benedetti, V. Gulizzi, A. Milazzo, *Advances in Boundary Element and Meshless Techniques XIX*, 11-16, (2018).
[24] I. Benedetti, M.H. Aliabadi, G. Davi. *International journal of solids and structures*, 45(7-8), 2355-2376, (2008).
[25] I. Benedetti, M.H. Aliabadi. *International journal for numerical methods in engineering*,84(9), 1038-1067, (2010).
[26] A. Froehlich, A. Brueckner-Foit and S. Weyer, In *Smart Structures and Materials 2000: Active Materials: Behavior and Mechanics*, **3992**, 279-288 (2000).
[27] J.Y. Li, M.L. Dunn and H. Ledbetter, *Journal of applied physics*, **86**(8), 4626-4634 (1999).
[28] E. Pan and F. Tonon. *International Journal of Solids and Structures*, **37**(6), 943-958 (2000).